LNC 96-102

Appendix D

Field Measurement and Mapping of Soil Salinity in Saline Seeps

K.R. Mankin, K.L. Ewing, M.D. Schrock, and G.J. Kluitenberg

Presented at the 1997 ASAE International Meeting

Paper No. 97 3145
An ASAE Meeting Presentation

FIELD MEASUREMENT AND MAPPING OF SOIL SALINITY IN SALINE SEEPS

by

K.R. Mankin, K.L. Ewing, M.D. Schrock
Research Assistant Professor, Undergraduate Student, Professor
Department of Biological and Agricultural Engineering

G.J. Kluitenberg
Associate Professor
Department of Agronomy

Kansas State University
Manhattan, Kansas 66506 USA

Written for Presentation at the
1997 ASAE Annual International Meeting
Sponsored by ASAE

Minneapolis Convention Center
Minneapolis, Minnesota
August 10-14, 1997

Summary:

A comparison of field measurements and resulting grid maps of soil electrical conductivity measured using several techniques is presented. Measurement techniques include: 1) a 4-electrode sensor using fixed-array configuration; 2) a mobile electrical conductivity sensor mounted on tillage tines; 3) EM 38; 4) EM 31; and 4) saturation extract conductivity from field soil samples. The various methods are compared for accuracy, reliability, and ease of use, particularly for field grid-type sampling for GIS applications. All methods adequately identified saline seep locations. EM31 apparently was able to determine seep recharge direction.

Keywords: GIS, GPS, Electromagnetic induction, Electrical conductivity.

Field Measurement and Mapping of Soil Salinity in Saline Seeps

Kyle R. Mankin, Kristi L. Ewing, Mark D. Schrock, and Gerard J. Kluitenberg

Summary: A comparison of field measurements and resulting grid maps of soil electrical conductivity measured using several techniques is presented. Measurement techniques include: 1) a 4-electrode sensor using fixed-array configuration; 2) a mobile electrical conductivity sensor mounted on tillage tines; 3) EM 38; 4) EM 31; and 4) saturation extract conductivity from field soil samples. The various methods are compared for accuracy, reliability, and ease of use, particularly for field grid-type sampling for GIS applications. All methods adequately identified saline seep locations. EM31 apparently was able to determine seep recharge direction.

INTRODUCTION

Accurate measurement and mapping of field soil conditions is becoming increasingly important to farmers. Precision agriculture technologies have matured to the point that many farmers have the ability to create detailed maps of crop yield with readily available global positioning system (GPS) hardware, geographic information system (GIS) software, and computer systems. Questions remain, however, as to what additional data can or should be collected at a reasonable cost to aid interpretation of this yield data, and how best to use and act upon these detailed maps.

Salinity can be an important soil parameter for agricultural fields. Management of soil salinity can be important not only for fields with saline seep conditions discussed in this paper, but also for fields under irrigation. Several technologies have been developed to map soil electrical conductivity in a relatively simple, detailed way without the need for intensive (and expensive) soil sampling. Among these technologies are electromagnetic induction (EM) and fixed-array 4-electrode conductivity sensors. Both types have been used to create the types of detailed maps needed for GIS.

Description of Saline Seeps

Saline seeps are an increasing concern in the dryland crop production areas of Kansas. The seeps, which range in size from a few square meters to 20 hectares, are growing in number, area, and severity. Due to their distributed nature, seeps often receive full inputs of tillage, fertilizer, and seed, even though no crop is produced. The seep areas are subject to serious wind and water erosion due to the total absence of vegetation under current management. Approximately 65,000 ha of south-central Kansas soils are mapped as saline/sodic, a number believed to be conservative because it is based on soil mapping work performed 30 years ago.

The term *saline seep* refers to an area of recent groundwater discharge on hillside locations in semiarid regions (Doering and Sandoval, 1976). Salts from upslope soils are leached by subsurface water movement and transported downslope to the seep area. Over time, salinization of the seep continues until once productive soils can no longer support crops. Seep development is related to the geology and climate of the region as well as the current system of crop production (Doering and Sandoval, 1976; Halvorson, 1988). In the Southern Plains region, the shift from native grass prairie to an annual winter wheat-fallow rotation has reduced the net plant water use, resulting in increased water movement downward through the soil. As the percolating water encounters a less permeable layer, lateral movement occurs until an outcrop area is reached, where the water evaporates and leaves behind the various salts that were accumulated along the flow path. The seeps typically go unnoticed for many years, until the salt concentration in the topsoil influences crop production.

The overall objectives of this project are to develop strategies to help farmers in Kansas remediate saline seeps using biological control methods. Accurate field salinity mapping for various profiles helps meet this goal by clearly defining seeps and the direction of seep recharge; tracking the size of the saline-affected areas over time, thereby monitoring the effectiveness of the remediation methods; providing preliminary indications of reclamation progress to help encourage the farmers to continue with the voluntary changes in management that are key to success of the remediation; and providing graphical illustration of the seep remediation process to assist with farmer education efforts. The specific objectives of this study were to:

1) evaluate and compare the ability of several soil-salinity measurement methods to provide detailed, accurate, field-scale salinity maps,
2) describe the vertical resolution and depth information provided by each sensor, and
3) determine which instruments are best suited to describing seep extent and recharge direction.

METHODS

Instrumentation

For each site, surface and profile soil salinity of both seep and recharge areas were measured and mapped. Extracted soil cores at 0-6, 6-12, 12-24, and 24-48 in. were used to estimate saturation extract conductivity, texture, and total soil water content. Saturation extract conductivity was measured by filtering a saturated mixture of soil and distilled water, and measuring the resulting solution extract with an electrical conductivity meter. Texture was analyzed for sand, silt, and clay percentages using a hydrometer method (Bouyoucos, 1962). Total soil moisture was taken as the difference between actual soil sample weight and dry weight after 72 hrs at 65 °C.

Fixed-Array, Four-Electrode Meters. Fixed-array conductivity sensors consist of four electrodes inserted along a straight line into the surface soil layer. A field generated across the outer two electrodes; the resulting resistance between the inner two electrodes is measured as a conductivity. A fixed array was constructed using a soil and water conductivity unit ([1]Model SCT-10, Martek Instruments, Inc., Irvine, CA) as a current source/resistance meter along with guidance from literature (Rhoades, 1971). The sequential electrode spacing was 0.127, 1.000, and 0.127 m. This unit was inserted 50 mm into the ground at each sampling point and read in units mmhos/cm. Temperature was corrected using a relationship provided by MARTEK (1989). Moisture and clay content were subsequently adjusted using Procedures II and III from Rhoades et al. (1990), with only minor modification. Resulting adjusted data are referred to herein as ECe-1 and ECe-2, respectively.

A second fixed-array sensor, a prototype Veris Technologies[1] mobile fixed-array unit, was tested on two of the three sites discussed in this paper. A key feature of this unit was that the four electrodes were chisel sweeps mounted behind a four-wheel drive cart. Data from the four electrodes were sampled on a near-continuous basis as the cart passed through the field, and saved in an on-board computer along with GPS coordinates for the sample locations. The two readings taken at each sample point had quoted effective depths of 0.3 m (1 ft) and 1.0 m (3 ft); other specific information regarding this instrument is proprietary at this time.

Electromagnetic Induction Meters. The electromagnetic induction meters used in this study were the EM38 and EM31, manufactured by Geonics Limited[1]. Details of their theory and operation are described elsewhere (McNeill, 1980a, 1986). Each meter provides limited vertical resolution and depth information. Meter resolution is approximately equal to the intercoil spacing of the meter. Observation depth is dependent upon intercoil spacing, transmission frequency, and coil orientation. The EM38 has an intercoil spacing of 3.2 ft, and theoretical observation depths of 2.5 and 5.0 ft in the horizontal and vertical dipole orientations, respectively (McNeill, 1986). The EM31 meter has an intercoil spacing of 12.7 ft, and theoretical observation depths of 10 and 20 ft in the horizontal and vertical dipole orientations, respectively (McNeill, 1980a). Values of apparent conductivity are expressed in mmhos/m.

Geographic Information System Analysis and Mapping

All soil properties were entered into a geographic information system (GIS) for analysis purposes. A Field Information System (FIS) was developed by Zhang et al. (1996). This windows-based GIS software analysis program allows entry of field spatial data into an array of data layers, and can integrate spatial data from different

[1] Trade names are used to provide specific information. Their mention does not constitute endorsement by Kansas State University.

sources with difference scales and resolutions. These data layers can then be manipulated, mapped, and analyzed. The program provides an interpolation function using user-defined resolution, and allows new layers to be created using arithmetic operations on existing data layers. FIS also enables the user to correlate corresponding points on any two layers using a standard correlation coefficient. In this study, data was transferred from field data sheets to a commercial spreadsheet program and then transformed into a format useable within FIS.

Statistics

Measurements from each instrument were compared against actual saturation extract conductivity values for each of the four depth layers. Multiple linear regression procedures were used (SAS, 1989). In addition, summary statistics were developed for each FIS layer at each site.

SITE CHARACTERISTICS

Saline seeps develop in response to an interaction of land management practices with local geomorphology and climate. An understanding of each is important to interpretation of the soil salinity profile measurements.

Geomorphology and Current Management

Site Rice 1. The site is located about two miles south and one mile east of Little River, KS. Slopes ranged from 0 to 3 percent with relief of 4.6 m. The surface slopes to the east and northeast toward the Little Arkansas River. A road parallels the field immediately to the south. The site is currently cropped to wheat. Soil delineations mapped within the site include phases of Geary, Hobbs, and Smolan soils (Horsch, 1974). The very deep, well-drained Geary (fine-silty, mixed, mesic Udic Argiustolls) and Smolan (fine, montmorillonitic, mesic Pachic Argiustolls) soils formed in loess on uplands. The very deep, well drained Hobbs soils (fine-silty, mixed, nonacid, mesic Mollic Ustifluvents) formed in alluvium on flood plains.

Site Rice 2. The site is located about one mile south and one mile east of Little River, KS. Slopes ranged from 0 to 7 percent with relief of 7.5 m. The surface slopes to the west and southwest toward the Little Arkansas River. The upland area was terraced and is currently cropped to wheat, while the area below the first terrace is planted to alfalfa. Soil delineations mapped within the site include phases of Detroit and Smolan soils (Horsch, 1974). The very deep, moderately well-drained Detroit soils (fine-silty, mixed, mesic Udic Argiustolls) formed in alluvium on flood plains, while the very deep, well-drained Smolan soils formed in loess on uplands.

Site Rice 3. The site is located about one mile north and one-half mile west of Little River, KS. Slopes ranged from 0 to 7 percent with relief of 8.2 m. The surface slopes to the east and southeast toward the Little Arkansas River. The upland area was terraced and is currently in CRP grasses, while the area below the first terrace is planted to wheat. Soil delineations mapped within the site include phases of Lancaster and Hobbs soils (Horsch, 1974). The moderately deep, moderately well-drained Lancaster soils (fine-silty, mixed, mesic Udic Argiustolls) formed in materials weathered from sandstone and shale on uplands. The very deep, well-drained Hobbs soils formed in alluvium on flood plains.

Climate

Normal average annual precipitation at the project sites in both Rice and Harper Counties falls between 27 and 28 in., with a 10% chance of receiving at least 36 in. and a 90% chance of receiving at least 18 in. Mean annual evaporation (precipitation minus runoff) is approximately 25 in., while the potential for evapotranspiration can be described as either 64 in. (Penman ET_o) or 56 in. (free water surface evaporation), significantly in excess of annual precipitation. The growing season ranges from 180 days in Northern Rice County to 200 days in southern Harper County. During this April to September period, Rice County receives approximately 75% of its annual precipitation while Harper County receives 71%. This timing of precipitation in relation to land management is important to seep development and reclamation (Mankin and Koelliker, 1997).

RESULTS AND DISCUSSION

Salinity data collected at each site using several methods is summarized in Table 1. Data was separated to compare samples taken within the saline seep and those take outside the seep area, where the seep area was roughly defined as the zone with poor or no crop growth. Within-seep means were significantly different from outside-seep means, as indicated by non-overlapping standard errors, except for two measurements at deeper levels (Rice 1: EM31-V; Rice 2: SE 24-48) and one shallow measurement (VER 0-36). This indicates that salinity was indeed higher beneath the plant-affected saline areas, and that all sensors had adequate precision and resolution to detect the increased salinity with the seep zone.

Besides being higher in the seep zone, salinity often exhibits an inversion with depth in saline seeps: salinity is higher near the surface than at depth. While no sites exhibited a clear inversion, at Rice 1, where the saline seep was the most clearly defined and well developed, the difference in salinity between seep and non-seep zones decreased with depth, as indicated by means of SE 0-6, 6-12, 12-24, and 24-48 (Table 1). The means also had the least variation (no significant differences) with depth at that site. By contrast, seeps at Rice 2 and Rice 3 were visually less distinctive and this was reflected in the data. Salinity increased significantly with depth within the seep at Rice 2 and Rice 3. It is also interesting to note that the salinity levels indicated by saturation extract data showed very little variation among sites, often demonstrating no significant differences among data taken at the same depths.

The lowest coefficient of variation (CV) was demonstrated by EM31 data, followed by EM38, and then the fixed-array sensors (Table 1). This may have been a reflection of the increased effective sampling depth of the two EM sensors compared to the fixed-array sensors. Samples which included a larger volume of soil would tend to dampen the effects of the more-variable surface salinity, and not vary a widely.

FIS was used to correlate the various instruments with the saturation extract conductivities, considered to represent "actual" salinity, and with each other. Results are presented in Tables 2, 3, and 4 for Rice 1, Rice 2, and Rice 3 sites. Each instrument most often had the highest correlation with other instruments with similar effective sampling depths, as anticipated. EM38-H and EM38-V were highly correlated at all sites (>0.93) while EM38-H was moderately correlated with raw and adjusted fixed-array values (>0.72). The Veris 0-12 in. depth sensor data had moderately-high correlation with the adjusted fixed-array data at Rice 1 (>0.83) but almost no correlation at Rice 2 (<0.10); this difference has not yet been explained. EM31 data measured deeper into the soil profile than all other instruments and had the lowest correlations in instrument-to-instrument comparisons (<0.81), with the best correlations coming with the moderately deep EM38-V.

Correlations between FIS data layers of individual sensors and specific saturation extract depths also yielded reasonable results. The fixed-array sensors tended to correlate better with the surface layers (primarily 0-6 in.) while the EM sensors generally had higher correlations with deeper layers (12-24 in. or deeper). For example, the highest correlations for both Veris sensors and the adjusted fixed-array sensors were all with the 0-6 in. saturation extract conductivity data, the raw fixed-array data and EM38-H had their highest correlations with the 6-12 in. layer, and the EM38-V and both EM31 orientations had their highest correlations in the 12-24 in. layer. It is also seen from this data that the correlations were highest for the fixed-array and EM38-H sensors, followed by EM38-V, Veris 0-12, EM31-H, Veris 0-36, and EM31-V, roughly in order of increasing depth.

FIS was also used to investigate correlations between individual sensors and weighted combinations of various depths of saturation extract conductivity. The 0-6 and 6-12 in. SE layers were averaged. The three FIS SE layers (0-12, 12-24, and 24-48 in.) were multiplied by various fractions and the result saved in a separate FIS layer. This weighted layer was then correlated with each instrument. An attempt was made to find the weighting that correlated well with the various instruments. Tables 2, 3, and 4 show the results of three such weightings in the lower portion of each table. In almost every case, better correlations were found when considering more than a single layer.

Correlations from FIS were corroborated by results from the multiple linear regression analysis (Table 5). This summary shows that only Rice 1 had significant r^2 correlation coefficients (> approx. 0.80), similar to the results of FIS. Measurements from EM31-H and VER36 were only moderately correlated, while EM31-V (the deepest instrument) was poorly correlated with the saturation extract data. Again, the deepest instruments showed the lowest r^2 coefficients. The significance of regression parameters for instruments with significant r^2 correlations was assessed (Table 5). The 0-6 in. SE parameters were highly significant for the fixed-array sensor and the Veris 0-12 in. sensor. The 6-12 in. SE parameter was also marginally significant for the Veris 0-12. The deeper Veris 0-36, which only had marginally significant r^2, had significant SE parameters in the 0-6, 6-12, and 12-24 in. depths. The only EM instrument with significant r^2 and regression parameter was the EM38-H with a marginally significant 0-6 in. SE parameter.

Though many of the instruments yielded poor correlations with actual data at some sites, useful information was nonetheless extracted from maps generated with their data. A complete set of maps from FIS is presented in Figures 1 through 13. All data is shown at the same horizontal scale, and data range grey-scales are the same for similar instruments to aid in comparisons between maps. North is toward the top of the page. Similar saline seep "hot spots" are seen in maps from all the sensors (Figs. 5-13), in agreement with saturation extract conductivity data (Figs. 1-4). All instruments are useful in delineating saline seep areas.

For remediation treatments to be located effectively, recharge direction for the seep must be clearly established. The deepest data, from the EM31-V (Fig. 13), appears to not only show the relative salinity hot spots in the same location as seen in shallower data, but also shows a "finger" of salinity from the bottom-center of the map to the upper left (north-west direction). A less-exaggerated finger also appears in the center of the map directed toward the west. These fingers may represent movement of higher salinity ground water toward the seeps. This hypothesis must be confirmed by analysis of deep soil cores and ground water monitoring wells.

CONCLUSIONS

Both fixed-array and EM sensors produced valuable data for evaluating saline seep extent and creating field-scale soil salinity maps. The Veris system was mobile and highly automated, and collected its data in a fraction of the time of the other methods which used hand-held instruments and collected data at measured grid-points. Use of a mile GPS unit like the Veris system would speed collection of data by the other methods considerably while probably retaining adequate resolution for this type of work.

None of the instruments had consistent, significant correlations with actual soil salinity, as indicated by saturation extract conductivity. When correlations were found, each instrument generally appeared to weigh the quoted depth range more heavily than other depth layers. The two adjustment equations for the fixed-array sensor from Rhoades et al. (1990) did not improve the correlations with actual salinity.

The EM31 was apparently able to discern recharge direction for the fields studied. This must be confirmed with more direct data. The shallower sensors apparently did not extend to the level of recharge flow.

The Field Information System (Zhang et al., 1996) proved useful for mapping and analyzing the field data. The system was relatively easy to use and allowed data taken at various grid spacings to be mapped with identical scale and resolution and subsequently analyzed. Several limitations found during input/output, mapping, and analysis are currently being addressed.

ACKNOWLEDGMENT

This material is based upon work supported by the Cooperative State Research, Education, and Extension Service, U.S. Department of Agriculture, under Cooperative Agreement No. 96-COOP-1-3020, and the Kansas Agricultural Experiment Station. The authors also appreciate the cooperation and generous support of Bob Murphy, Gary Parks, and Jim Doolittle of NRCS, and Colin Christy and Eric Lund of Veris Technologies/GeoProbe Systems during various phases of this project.

REFERENCES

ASA/SSSA. 1986. Methods of Soil Analysis, Part 1. Physical and Mineralogical Methods. G.W. Gee and J.W. Bauder (ed.) American Society of Agronomy/Soil Sciences Society of America. Agronomy Monograph No. 9, 2nd ed.

Bouyoucos, G.J. 1962. Hydrometer method improved for making particle size analyses of soils. Agron. J. 54:464-465.

Doering, E.J. and F.M. Sandoval. 1976. Hydrology of saline seeps in the Northern Great Plains. Trans. ASAE 19:856-861, 865.

Halvorson, A.D. 1988. Role of cropping systems in environmental quality: Saline seep control. p. 179-191. *In* W.L. Hargrove et al. (ed.) Cropping strategies for efficient use of water and nitrogen. ASA Spec. Publ. 51. ASA, CSSA, and SSSA, Madison, WI.

Horsch, M.L. 1974. Soil survey of Rice County, Kansas. USDA-Soil Conservation Service. U.S. Government Printing Office. Washington, D.C. 63 pp.

Mankin, K.R. and J.K. Koelliker. 1997. Phytoremediation of saline seeps by hydrologic modification. Presented at ASAE Annual International Meeting, Minneapolis, Minn., 10-14 August, Paper No. 97-2013. American Society of Agricultural Engineers, St. Joseph, MI.

MARTEK. 1989. Soil and water conductivity/temperature analyzer, Model SCT-10. Operations Manual. Martek Instruments, Inc. Irvine, CA.

McNeill, J.D. 1980a. Electromagnetic terrain conductivity measurement at low induction numbers. Technical Note TN-6. Geonics Limited, Mississauga, Ontario. 15 pp.

McNeill, J.D. 1986. Geonics EM38 ground conductivity meter operating instructions and survey interpretation techniques. Technical Note TN-21. Geonics Limited, Mississauga, Ontario. 16 pp.

Rhoades, J.D., P.J. Shouse, W.J. Alves, N.A. Manteghi, and S.M. Lesch. 1990. Determining soil salinity from soil electrical conductivity using different models and estimates. Soil Sci. Soc. of Amer. J. 54:46-54.

Zhang, N., E. Runquist, M. Schrock, J. Havlin, G. Kluitenberg, and C. Redula. 1996. Making GIS a versatile analytical tool for research in precision farming. p. 387-392. *In* C. Lokhorst, A.J. Udink tenCate, and A.A. Dijkhuizen (ed.) Information and Communication Technology Application in Agriculture: State of the Art and Future Perspectives. Proceedings of the 6th International Congress for Computer Technology in Agriculture. Wageningen, The Netherlands.

Table 1. Descriptive Statistics for each measurement at three sites.

Rice 1

	SE 0-6	SE 6-12	SE 12-24	SE 24-48	EM 38 H.	EM 38 V.	EM 31 H.	EM 31 V.	F.A.(raw)	ECe 1	ECe 2	VER.0-12	VER.0-36
							within seep						
n	6	6	6	6	6	6	6	6	6	6	6	6	6
mean	2.47	2.48	3.88	2.72	111.67	117.00	103.64	100.07	16.14	108.93	109.44	109.10	113.05
median	1.94	2.78	4.37	2.87	120.00	125.00	106.95	99.10	16.84	111.68	112.23	105.72	96.42
High	5.23	4.16	6.83	4.28	145.00	140.00	116.64	109.97	26.63	175.82	176.36	202.54	177.21
Low	0.79	0.61	0.77	1.02	67.00	80.00	84.80	94.18	7.07	47.67	48.12	17.83	51.49
Std. Dev.	1.57	1.42	2.35	1.22	27.75	22.03	10.46	5.02	7.12	49.55	49.53	68.66	45.36
Std. Err.	0.64	0.58	0.96	0.50	11.33	8.99	4.27	2.05	2.91	20.23	20.22	28.03	18.52
Skewness	0.90	-0.38	-0.32	-0.18	-0.66	-0.76	-0.90	1.29	-0.01	-0.05	-0.06	0.08	0.44
CV (%)	63.53	57.36	60.66	44.85	24.85	18.83	10.09	5.02	44.09	45.49	45.26	62.93	40.12
							outside seep						
n	18	18	18	18	18	18	18	18	18	18	18	18	18
mean	0.22	0.18	0.69	1.64	52.83	72.50	88.26	96.42	4.00	24.43	25.02	31.87	68.37
median	0.20	0.12	0.19	1.06	54.50	73.50	87.97	98.44	3.53	20.44	21.12	23.63	54.55
High	0.66	0.74	2.84	4.95	80.00	104.00	109.94	107.20	9.44	67.29	67.64	78.93	151.87
Low	0.10	0.06	0.05	0.12	33.00	46.00	68.44	82.51	2.23	11.97	12.61	17.58	30.38
Std. Dev.	0.11	0.16	0.83	1.56	13.90	17.14	12.40	6.74	1.66	12.34	12.28	16.15	36.53
Std. Err.	0.03	0.04	0.20	0.37	3.28	4.04	2.92	1.59	0.39	2.91	2.90	3.81	8.61
Skewness	3.41	2.64	1.34	0.91	0.43	0.19	0.24	-0.48	2.08	2.45	2.44	1.69	1.08
CV (%)	52.66	84.98	120.85	95.33	26.31	23.65	14.05	6.99	41.45	50.50	49.09	50.68	53.42

Rice 2

	SE 0-6	SE 6-12	SE 12-24	SE 24-48	EM 38 H.	EM 38 V.	EM 31 H.	EM 31 V.	F.A.(raw)	ECe 1	ECe 2	VER.0-12	VER.0-36
							within seep						
n	3	3	3	3	34	34	39	39	31	31	31	39	39
mean	0.41	1.33	2.48	1.68	63.94	79.76	90.83	91.78	7.72	52.51	52.99	55.08	81.89
median	0.49	1.25	2.67	1.70	62.50	78.50	91.40	90.20	7.45	50.22	50.73	53.63	83.43
High	0.54	1.62	3.88	2.77	91.00	110.00	111.00	103.40	15.13	108.22	108.71	210.63	120.43
Low	0.21	1.11	0.89	0.58	40.00	58.00	70.60	76.60	4.93	32.28	32.76	13.06	41.37
Std. Dev.	0.15	0.22	1.23	0.89	10.85	12.54	9.41	5.97	1.93	14.34	14.34	28.23	17.23
Std. Err.	0.08	0.12	0.71	0.52	1.86	2.15	1.51	0.96	0.35	2.58	2.58	4.52	2.76
Skewness	3.84	3.47	4.26	4.42	-1.49	-1.56	0.06	0.03	-0.47	-0.30	-0.32	4.31	-0.12
CV (%)	35.13	16.22	49.52	53.12	16.98	15.72	10.36	6.51	25.03	27.32	27.07	51.25	21.05
							outside seep						
n	3	3	3	3	38	38	81	81	29	29	29	81	81
mean	0.18	0.13	0.17	1.78	50.26	65.34	76.20	82.30	4.01	26.16	26.63	45.52	57.56
median	0.20	0.14	0.14	0.26	51.00	64.50	76.80	81.60	3.55	22.85	23.33	33.95	51.41
High	0.20	0.14	0.32	4.91	65.00	90.00	111.20	103.40	7.38	49.59	50.06	364.36	147.19
Low	0.14	0.12	0.06	0.18	29.00	39.00	50.40	64.20	1.05	6.09	6.49	13.88	21.55
Std. Dev.	0.03	0.01	0.11	2.21	9.50	12.77	12.17	8.76	1.84	12.63	12.63	55.29	26.25
Std. Err.	0.02	0.01	0.06	1.28	1.54	2.07	1.35	0.97	0.34	2.34	2.35	6.14	2.92
Skewness	5.18	5.04	7.15	8.95	0.30	0.32	0.12	0.11	1.36	1.41	1.39	5.02	0.90
CV (%)	15.71	7.07	62.73	123.99	18.90	19.54	15.98	10.65	45.93	48.27	47.42	121.47	45.60

Rice 3

	SE 0-6	SE 6-12	SE 12-24	SE 24-48	EM 38 H.	EM 38 V.	EM 31 H.	EM 31 V.
							within seep	
n	2	2	2	2	16	16	18	18
mean	1.58	1.23	1.68	2.18	73.19	110.13	142.47	166.33
median	1.58	1.23	1.68	2.18	69.50	107.50	141.00	171.50
High	1.94	1.33	1.91	2.66	104.00	146.00	183.80	202.80
Low	1.21	1.13	1.45	1.70	64.00	94.00	108.00	114.80
Std. Dev.	0.37	0.10	0.23	0.48	9.81	12.28	18.52	19.48
Std. Err.	0.26	0.07	0.16	0.34	2.45	3.07	4.37	4.59
Skewness	2.99	2.74	2.81	2.97	-1.90	-2.15	0.34	-0.89
CV (%)	23.17	8.13	13.69	22.02	13.40	11.15	13.00	11.71
							outside seep	
n	4	4	4	4	54	54	81	81
mean	0.27	0.14	0.15	0.27	42.87	61.98	86.72	111.82
median	0.28	0.14	0.16	0.19	40.00	61.00	87.80	114.80
High	0.30	0.20	0.17	0.53	78.00	94.00	130.60	168.00
Low	0.23	0.09	0.12	0.17	30.00	37.00	49.00	47.20
Std. Dev.	0.03	0.04	0.02	0.15	9.19	14.55	20.67	27.89
Std. Err.	0.01	0.02	0.01	0.08	1.25	1.98	2.30	3.10
Skewness	4.30	4.79	4.34	6.28	-0.28	-0.27	0.24	-0.15
CV (%)	9.49	28.12	12.47	55.74	21.44	23.48	23.83	24.94

Abbreviated headings are, respectively: Saturation Extract (SE) for 0-6, 6-12, 12-24, and 24-48 in.depths; Electromagnetic (EM) Induction meter, model 38, horizontal and vertical dipole orientations; EM 31 horizontal and vertical dipole orientations; Measured Fixed Array; Effective EC calculated by Methods 1 and 2; and Veris Mobile Unit for 0-12 and 0-36 in.depths.

Table 2. Correlation Coefficients using FIS for **Rice 1**.

	SE 0-6	SE 6-12	SE 12-24	SE 24-48	EM 38 H.	EM 38 V.	EM 31 H.	EM 31 V.	Raw F.A.	ECe 1	ECe 2	Veris 0-12	Veris 0-36
SE 0-6 in.†	--------												
SE 6-12 in.	0.8448	--------											
SE 12-24 in.	0.6634	0.9201	---------										
SE 24-48 in.	0.3599	0.4996	0.6994	---------									
EM 38 H.	0.8028	0.9237	0.9194	0.6450	---------								
EM 38 V.	0.6897	0.8469	0.9044	0.7277	0.9622	---------							
EM 31 H.	0.5654	0.6312	0.7249	0.7185	0.8096	0.8496	---------						
EM 31 V.	0.1078	0.2162	0.2589	0.1899	0.4029	0.4561	0.5659	---------					
Raw F.A.	0.9357	0.9496	0.8427	0.4978	0.9285	0.8361	0.6773	0.2617	---------				
ECe 1	0.9420	0.8573	0.7364	0.5026	0.8877	0.7941	0.7440	0.3065	0.9606	---------			
ECe 2	0.9470	0.8609	0.7380	0.4944	0.8912	0.7966	0.7419	0.2903	0.9634	0.9982	---------		
Veris 0-12 in.	0.8271	0.5250	0.3682	0.2454	0.6245	0.5223	0.5823	0.2429	0.7132	0.8359	0.8412	---------	
Veris 0-36 in.	0.6149	0.4325	0.4355	0.4016	0.6264	0.6137	0.7626	0.3507	0.5697	0.6927	0.7017	0.8216	--------
$0.91D_1+0.06D_2+0.03D_3$ ‡	0.9440	0.9713	0.8625	0.5055	0.9211	0.8332	0.6566	0.1829	0.9838	0.9342	0.9381	0.6812	0.5492
$0.60D_1+0.40D_2$	0.8440	0.9834	0.9587	0.6060	0.9523	0.8945	0.7080	0.2257	0.9520	0.8718	0.8750	0.5546	0.5116
$0.29D_1+0.50D_2+0.21D_3$	0.7246	0.9207	0.9857	0.7731	0.9385	0.9248	0.7671	0.2470	0.8753	0.7977	0.7980	0.4510	0.4930

† Abbreviated headings are, respectively: Saturation Extract (SE) for 0-6, 6-12, 12-24, and 24-48 in.depths; Electromagnetic (EM) Induction meter, model 38, horizontal and vertical dipole orientations; EM 31 horizontal and vertical dipole orientations; Measured Fixed Array; Effective EC calculated by Methods 1 and 2; and Veris Mobile Unit for 0-12 and 0-36 in.depths.

‡ D_1 = Average of 0-6 and 6-12 in. depths SE; D_2 = 12-24 in. depth SE; D_3 = 24-48 in. depth SE.

Table 3. Correlation Coefficients using FIS for **Rice 2**.

	SE 0-6	SE 6-12	SE 12-24	SE 24-48	EM 38 H.	EM 38 V.	EM 31 H.	EM 31 V.	Raw F.A.	ECe 1	ECe 2	Veris 0-12	Veris 0-36
SE 0-6 in.†	--------												
SE 6-12 in.	0.9330	--------											
SE 12-24 in.	0.7305	0.9261	---------										
SE 24-48 in.	-0.8062	-0.7434	-0.5401	---------									
EM 38 H.	0.6034	0.5868	0.4871	-0.4324	---------								
EM 38 V.	0.4987	0.4763	0.3832	-0.3662	0.9332	---------							
EM 31 H.	0.3775	0.3112	0.1973	-0.4587	0.7117	0.7273	---------						
EM 31 V.	0.3162	0.2053	0.5825	-0.4323	0.5380	0.5156	0.8097	---------					
Raw F.A.	0.6532	0.5869	0.4428	-0.4327	0.7326	0.5494	0.5237	0.4700	---------				
ECe 1	0.6289	0.5586	0.4153	-0.2477	0.7263	0.5441	0.5239	0.4698	0.9992	---------			
ECe 2	0.6290	0.5587	0.4153	-0.2854	0.7265	0.5443	0.5241	0.4700	0.9992	1.000	---------		
Veris 0-12 in.	0.6733	0.1104	0.1329	-0.0675	0.1478	0.1199	0.0906	0.1069	0.0973	0.0952	0.0953	---------	
Veris 0-36 in.	0.3763	0.3554	0.2906	-0.1825	0.6496	0.6536	0.7200	0.4143	0.4889	0.4895	0.4895	0.2312	---------
$0.91D_1+0.06D_2+0.03D_3$ ‡	0.9194	0.9987	0.9393	-0.7120	0.5896	0.4774	0.3123	0.1960	0.5858	0.5578	0.5579	0.1156	0.3598
$0.60D_1+0.40D_2$	0.8145	0.9680	0.9911	-0.6195	0.5307	0.4225	0.2409	0.1110	0.5017	0.4734	0.4735	0.1269	0.3188
$0.29D_1+0.50D_2+0.21D_3$	0.7021	0.9044	0.9909	-0.4640	0.5064	0.3995	0.2267	0.0609	0.4568	0.4310	0.4310	0.1463	0.3114

† Abbreviated headings are, respectively: Saturation Extract (SE) for 0-6, 6-12, 12-24, and 24-48 in.depths; Electromagnetic (EM) Induction meter, model 38, horizontal and vertical dipole orientations; EM 31 horizontal and vertical dipole orientations; Measured Fixed Array; Effective EC calculated by Methods 1 and 2; and Veris Mobile Unit for 0-12 and 0-36 in.depths.

‡ D_1 = Average of 0-6 and 6-12 in. depths SE; D_2 = 12-24 in. depth SE; D_3 = 24-48 in. depth SE.

Table 4. Correlation Coefficients using FIS for **Rice 3**.

	SE 0-6	SE 6-12	SE 12-24	SE 24-48	EM 38 H.	EM 38 V.	EM 31 H.	EM 31 V.
SE 0-6 in.†	--------							
SE 6-12 in.	0.9914	--------						
SE 12-24 in.	0.9964	0.9987	---------					
SE 24-48 in.	0.9928	0.9903	0.9911	---------				
EM 38 H.	0.4674	0.4859	0.4740	0.5198	---------			
EM 38 V.	0.5021	0.5154	0.5058	0.5533	0.9663	---------		
EM 31 H.	0.3404	0.3532	0.3451	0.3801	0.7484	0.7956	--------	
EM 31 V.	0.3361	0.3511	0.3415	0.3831	0.7325	0.8012	0.9148	---------
$0.91D_1+0.06D_2+0.03D_3$ ‡	0.9982	0.9975	0.9995	0.9941	0.4785	0.5110	0.3483	0.3452
$0.60D_1+0.40D_2$	0.9975	0.9981	0.9999	0.9926	0.4755	0.5077	0.3461	0.3426
$0.29D_1+0.50D_2+0.21D_3$	0.7775	0.9978	0.9992	0.9956	0.4874	0.5198	0.3552	0.3534

† Abbreviated headings are, respectively: Saturation Extract (SE) for 0-6, 6-12, 12-24, and 24-48 in.depths; Electromagnetic (EM) Induction meter, model 38, horizontal and vertical dipole orientations; and EM 31 horizontal and vertical dipole orientations.

‡ D_1 = Average of 0-6 and 6-12 in. depths SE; D_2 = 12-24 in. depth SE; D_3 = 24-48 in. depth SE.

Table 5. Correlation coefficients (r^2) and multiple linear regression p-values for each measurement at three sites.

	EM38-H	EM38-V	EM31-H	EM31-V	FA-Raw	ECe-1	ECe-2	VER-12	VER-36
Rice 1									
r^2	0.92	0.86	0.66	0.07	0.97	0.96	0.96	0.80	0.58
SE 0-6	0.077	0.352	0.1384	0.770	0.0001	0.0001	0.0001	0.0001	0.0009
SE 6-12	0.704	0.999	0.334	0.921	0.124	0.464	0.457	0.060	0.017
SE 12-24	0.116	0.149	0.2068	0.817	0.443	0.233	0.234	0.412	0.049
SE 24-48	0.391	0.159	0.201	0.964	0.709	0.855	0.859	0.885	0.704
Rice 2									
r^2	0.46	0.33	0.19	0.10	0.16	0.15	0.15	0.024	0.19
SE 0-6	0.053	0.047	0.564	0.813	0.644	0.604	0.606	0.987	0.140
SE 6-12	0.002	0.004	0.169	0.380	0.892	0.957	0.954	0.993	0.036
SE 12-24	0.003	0.004	0.121	0.241	0.763	0.809	0.805	0.868	0.040
SE 24-48	0.0001	0.0004	0.001	0.262	0.545	0.545	0.549	0.479	0.007
Rice 3									
r^2	0.37	0.43	0.26	0.31	--	--	--	--	--
SE 0-6	0.068	0.016	0.059	0.025	--	--	--	--	--
SE 6-12	0.398	0.108	0.297	0.200	--	--	--	--	--
SE 12-24	0.426	0.147	0.319	0.230	--	--	--	--	--
SE 24-48	0.001	0.0001	0.0009	0.0001	--	--	--	--	--

Interp. Results for SE6RSS.PTS (4 interp. points) [Rice1 South Seep Topography]

Sat. Extract Cond., 0.00–0.15 m, Rice 1

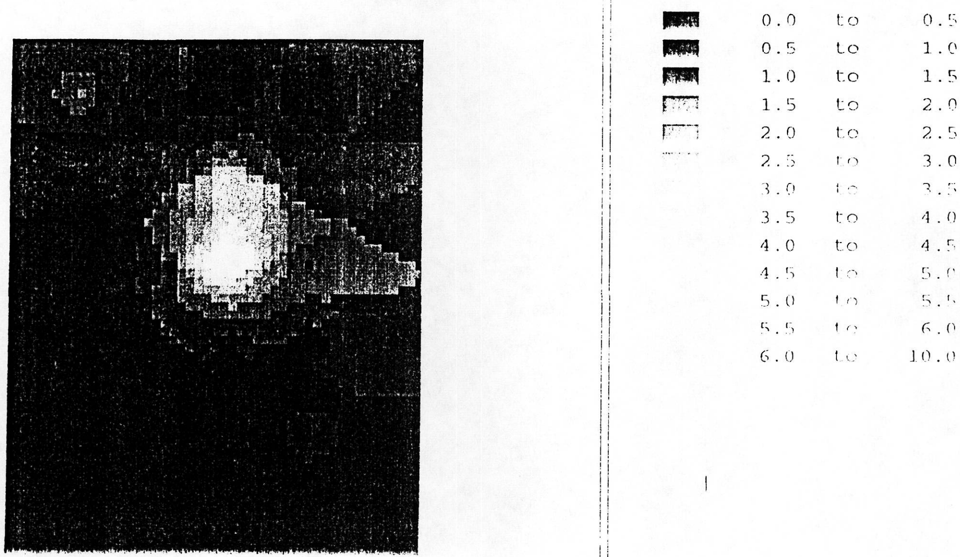

Figure 1.

Interp. Results for SE12RSS.PTS (4 interp. points) [Rice1 South Seep Topography]

Sat. Extract Cond., 0.15–0.30 m, Rice 1

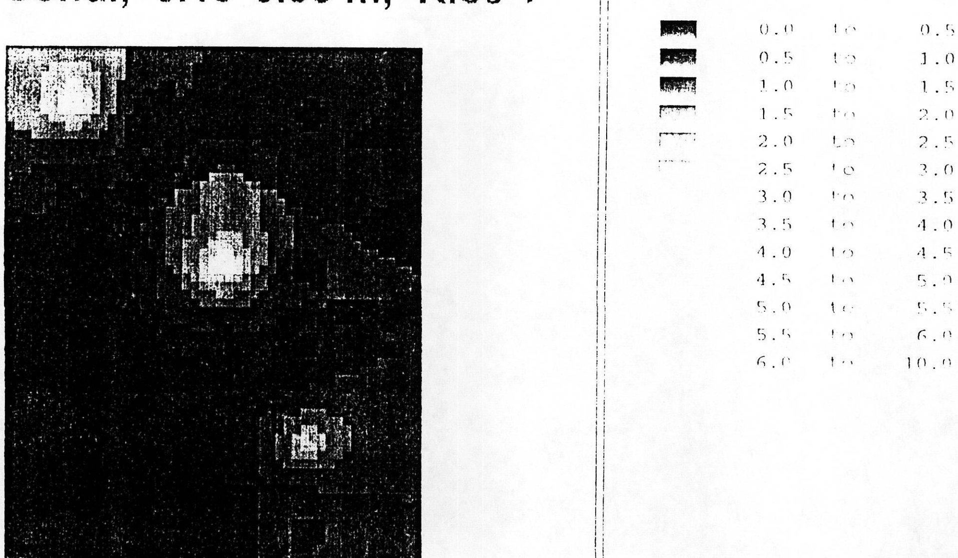

Figure 2.

Interp. Results for SE24RSS.PTS (4 interp. points) [Rice1 South Seep Topography]

Sat. Extract Cond., 0.30–0.60 m, Rice 1

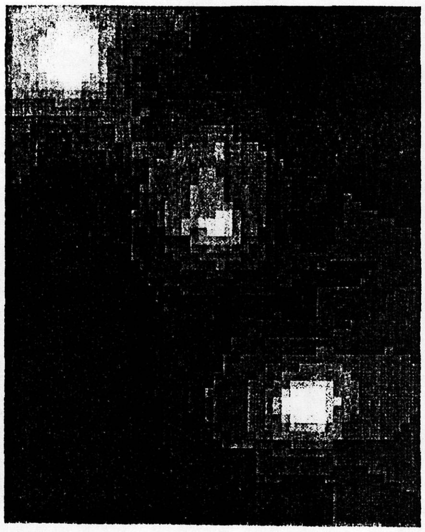

Figure 3.

Interp. Results for SE48RSS.PTS (4 interp. points) [Rice1 South Seep Topography]

Sat. Extract Cond., 0.60–1.20 m, Rice 1

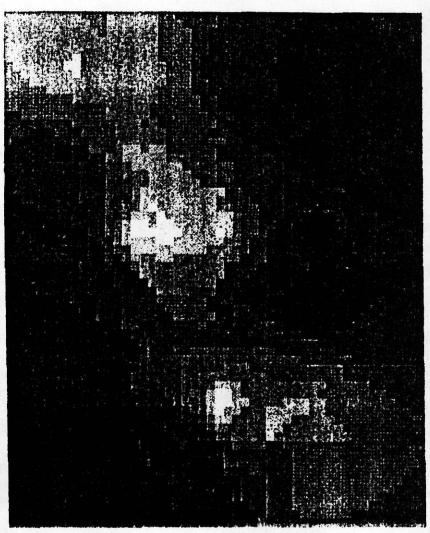

Figure 4.

Interp. Results for WA24RSS.PTS (4 interp. points) [Rice1 South Seep Topography]

Fixed Array, 0.0–0.3 m, Rice 1

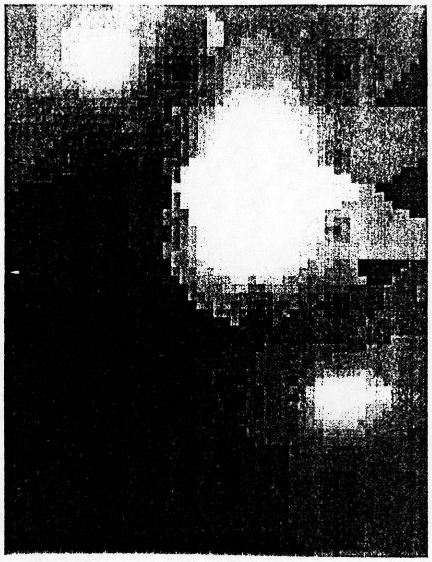

0	to	1
1	to	2
2	to	3
3	to	4
4	to	5
5	to	6
6	to	7
7	to	8
8	to	9
9	to	10
10	to	11
11	to	12
12	to	13
13	to	14
14	to	15
15	to	30

Figure 5.

Interp. Results for R1ADJWA.PTS (4 interp. points) [Rice1 South Seep Topography]

ECe-1, 0.0–0.30 m, Rice 1

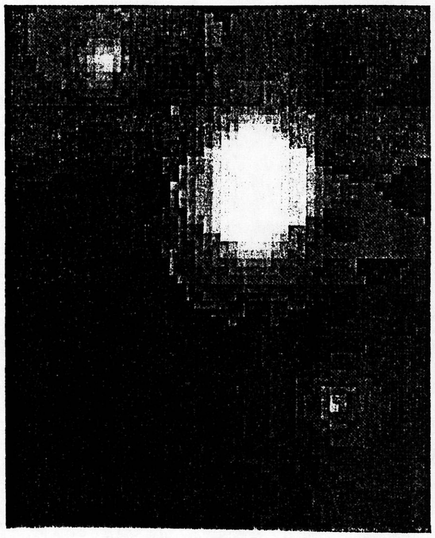

0	to	10
10	to	20
20	to	30
30	to	40
40	to	50
50	to	60
60	to	70
70	to	80
80	to	90
90	to	100
100	to	110
110	to	120
120	to	130
130	to	140
140	to	150
150	to	300

Figure 6.

Interp. Results for R1ADJWA2.PTS (4 interp. points) [Rice1 South Seep Topography]

ECe-2, 0.0–0.30 m, Rice 1

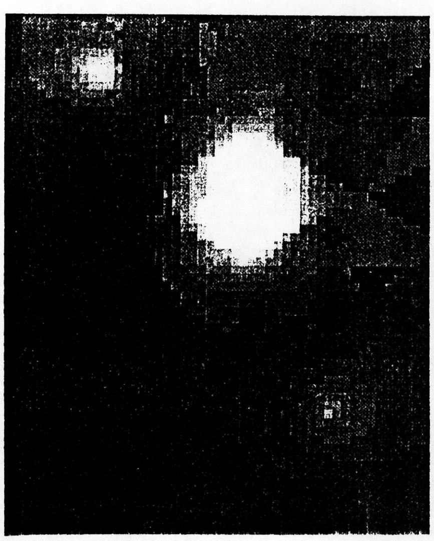

0	to	10
10	to	20
20	to	30
30	to	40
40	to	50
50	to	60
60	to	70
70	to	80
80	to	90
90	to	100
100	to	110
110	to	120
120	to	130
130	to	140
140	to	150
150	to	300

Figure 7.

Interp. Results for VERIS11.PTS (4 interp. points) [Rice1 South Seep Topography]

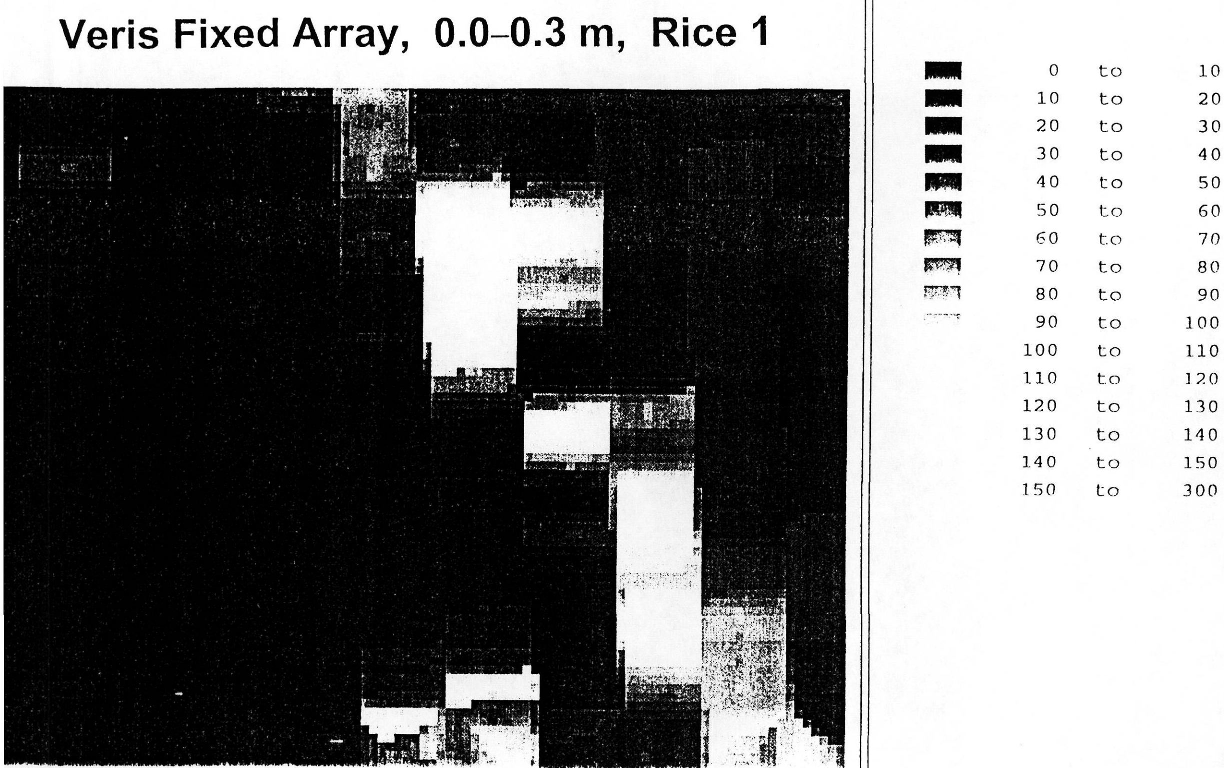

Figure 8.

Interp. Results for VERIS13.PTS (4 interp. points) [Rice1 South Seep Topography]

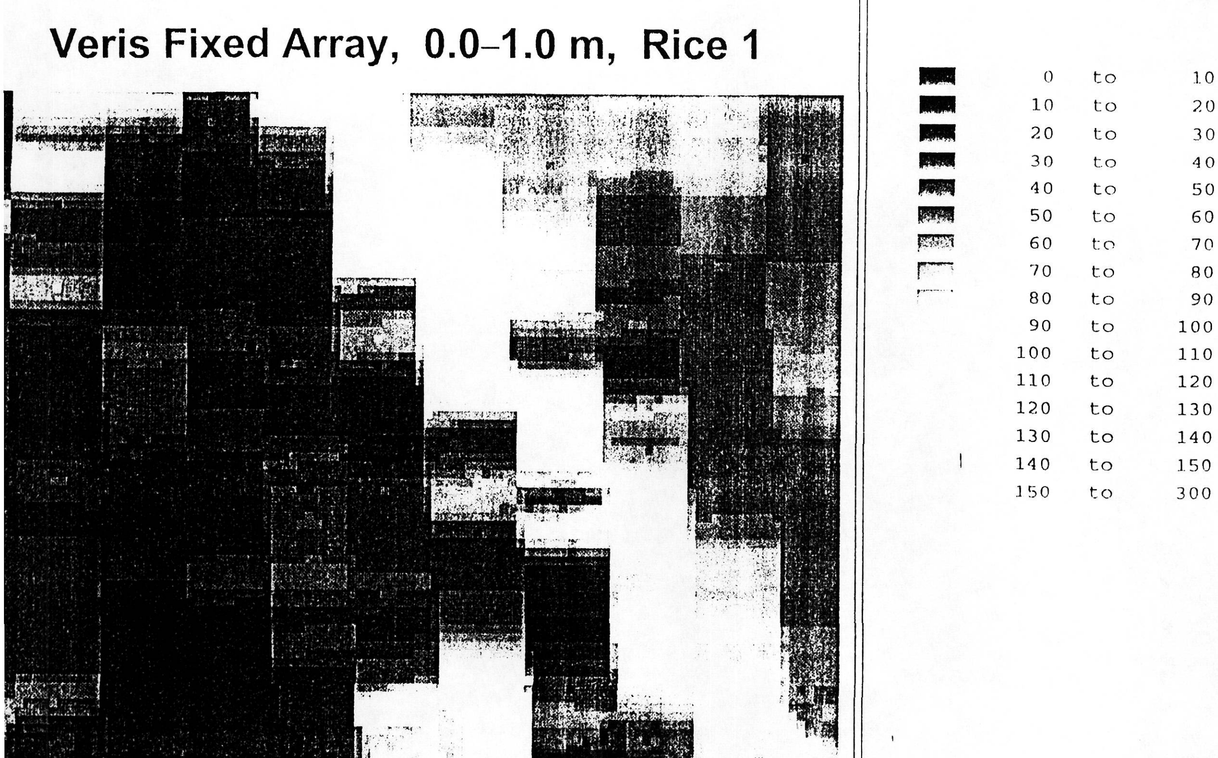

Figure 9.

Interp. Results for EM38SS24.PTS (4 interp. points) [Rice1 South Seep Topography]

EM38-Horizontal, 0.75 m, Rice 1

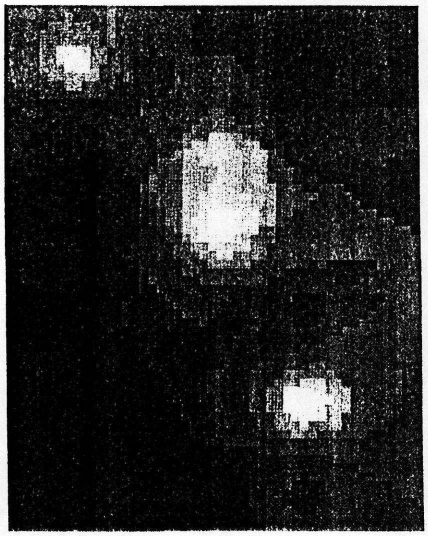

0	to	10
10	to	20
20	to	30
30	to	40
40	to	50
50	to	60
60	to	70
70	to	80
80	to	90
90	to	100
100	to	110
110	to	120
120	to	130
130	to	140
140	to	150
150	to	300

Figure 10.

Interp. Results for EM38V48.PTS (4 interp. points) [Rice1 South Seep Topography]

EM38-Vertical, 1.5 m, Rice 1

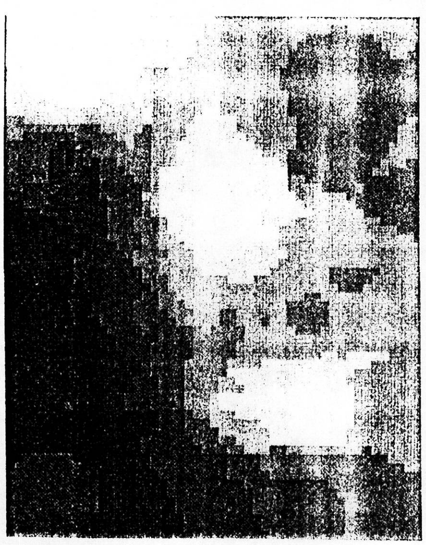

0	to	10
10	to	20
20	to	30
30	to	40
40	to	50
50	to	60
60	to	70
70	to	80
80	to	90
90	to	100
100	to	110
110	to	120
120	to	130
130	to	140
140	to	150
150	to	300

Figure 11.

Interp. Results for RC131H.PTS (1 interp. points) [Rice1 South Seep Topography]

EM31–Horizontal, 3.0 m, Rice 1

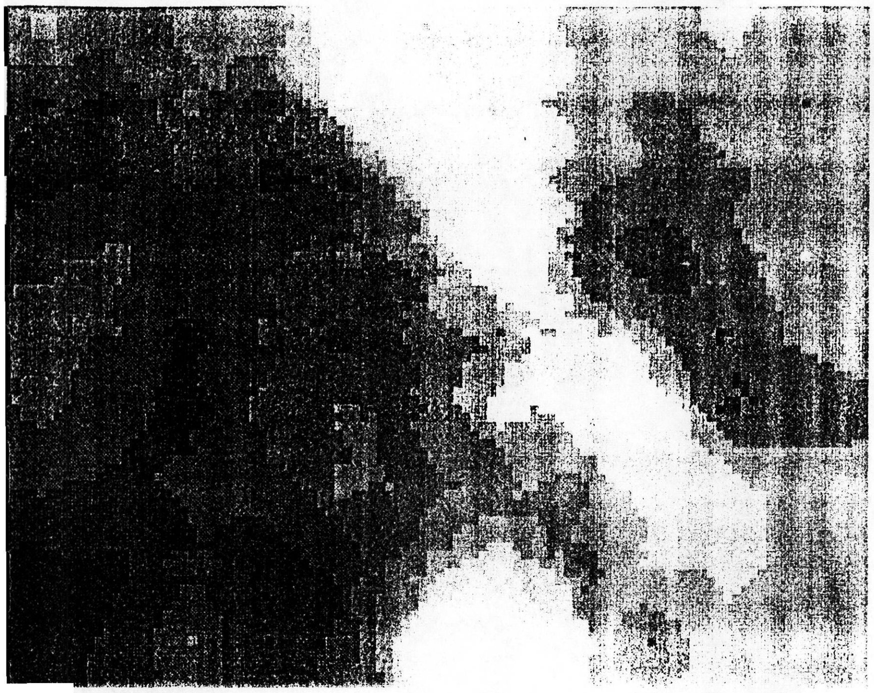

0	to	10
10	to	20
20	to	30
30	to	40
40	to	50
50	to	60
60	to	70
70	to	80
80	to	90
90	to	100
100	to	110
110	to	120
120	to	130
130	to	140
140	to	150
150	to	300

Figure 12.

Interp. Results for RC131V.PTS (1 interp. points) [Rice1 South Seep Topography]

EM31–Vertical, 6.0 m, Rice 1

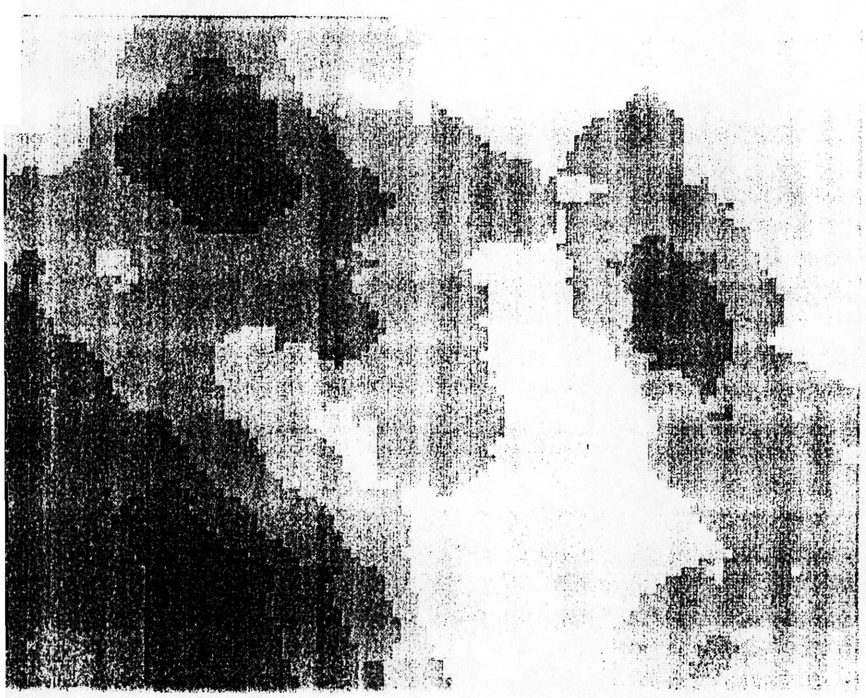

0	to	10
10	to	20
20	to	30
30	to	40
40	to	50
50	to	60
60	to	70
70	to	80
80	to	90
90	to	100
100	to	110
110	to	120
120	to	130
130	to	140
140	to	150
150	to	300

Figure 13.